

# **Dynamical Behavior of Carbon Nanotubes – Modeling, Simulations and Experiments**

NSF NIRT Grant 0303674

PIs: **Subrata Mukherjee<sup>1</sup>, Tomas Arias<sup>2</sup>, Paul McEuen<sup>2</sup>**

<sup>1</sup>Department of Theoretical and Applied Mechanics and <sup>2</sup>Department of Physics  
Cornell University

## **Project Objectives and Methodology**

Carbon nanotubes (CNTs) possess remarkable properties. They are very stiff and very strong, yet ductile. They can be conducting or semiconducting, depending on their chirality. Possible applications of CNTs include diverse areas such as conductive and high strength composites, energy storage and conversion devices, sensors, field emission displays and radiation sources, nanometer sized semiconductor devices, probes and interconnects. This project is concerned with a fundamental modeling, numerical and experimental study of the dynamical response of carbon nanotubes.

Primary project objectives:

- A hierarchical modeling approach is proposed here in which standard continuum mechanics, enriched continuum mechanics and molecular dynamics are being used to study the dynamical response of CNTs.
- Experiments are being carried out to measure natural frequencies and quality factors of suspended nanotubes. Measured values are being compared with simulations based on different models described above.
- Nanoscale devices such as tunable high frequency oscillators, transistors and ultrasensitive mass and force transducers will be built.

## **Research Progress**

### **1. Enriched continuum mechanics model for CNTs [1]:**

Development of a nonlinear atomistic-continuum constitutive framework is currently underway to characterize the mechanical behavior of single-walled nanotubes. Following the constitutive model developed by Zhang et al.[2], Mukherjee's group has successfully extracted the extensional and torsional stiffnesses ( $E_t$  and  $G_t$  respectively, where  $E$ : Young's modulus,  $G$ : Torsional modulus,  $t$ : nanotube wall thickness) of representative armchair, zigzag and chiral nanotubes. Using the Tersoff-Brenner multi-body interatomic potential for carbon, the elasticity tensor (in the context of a continuum analysis) is obtained from an appropriate definition of the strain energy density function. Expressions for the extensional and torsional stiffnesses are then derived, and the numerical values (given in Table 1) are obtained at the onset of deformation. Consistent values obtained corresponding to these material properties indicate that they do not depend strongly on the chirality of the nanotube (Saito et al.[3]) except for certain cases. The aforementioned framework contains the capability to extract constitutive relations at intermediate stages of deformation and is expected to be an important component of further mechanical analyses. Also encouraging is the fact that the relative magnitudes of the torsional and extensional stiffnesses fall within the well known range in continuum mechanics.

2. A tunable carbon nanotube electromechanical oscillator [4]:

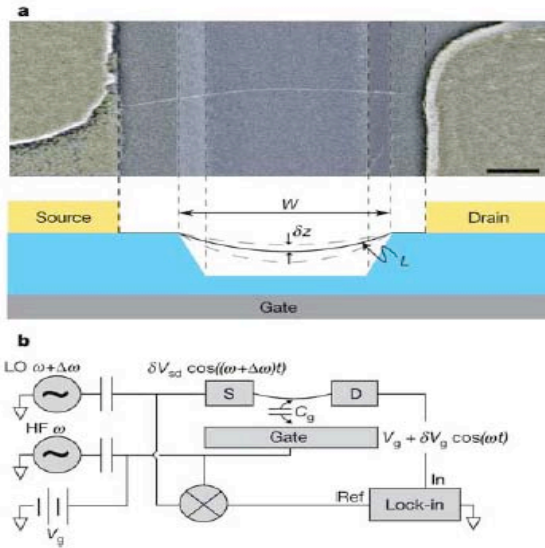


**Figure 1** Device geometry and diagram of experimental set-up. **a**, A false-colour SEM image of a suspended device (top) and a schematic of device geometry (bottom). Scale bar, 300 nm. Metal electrodes (Au/Cr) are shown in yellow, and the silicon oxide surface in grey. The sides of the trench, typically 1.2–1.5  $\mu\text{m}$  wide and 500 nm deep, are marked with dashed lines. A suspended nanotube can be seen bridging the trench. CVD growth is known to produce predominantly single- and double-walled nanotubes, but we did not perform detailed studies of the number of walls for the nanotubes on our samples. **b**, A diagram of the experimental set-up. A local oscillator (LO) voltage  $\delta V_{sd} \cos((\omega + \Delta\omega)t)$  (usually around 7 mV) is applied to the source (S) electrode at a frequency offset from the high frequency (HF) gate voltage signal  $\delta V_g \cos(\omega t)$  by an intermediate frequency  $\Delta\omega$  of 10 kHz. The current from the nanotube is detected by a lock-in amplifier through the drain electrode (D), at  $\Delta\omega$ , with time constant of 100ms.

Modeling and simulation of electrical actuation and detection of guitar-string oscillation modes of doubly-clamped CNT oscillators have just been reported in an article in the journal *Nature* [4]. It is shown here that the resonance frequencies can be widely tuned and that the devices can be used to transduce very small forces. The device geometry and experimental set-up are shown in Figure 1. The CNTs are grown by Chemical Vapor Deposition (CVD) and are suspended over a trench (typically 1.2-1.5  $\mu\text{m}$  wide and 500 nm deep) between two metal (Au/Cr) electrodes. The measurement is done in a vacuum chamber. Actuation and detection of the nanotube motion is carried out by using electrostatic interaction with the gate electrode under the tube. Transistor properties of

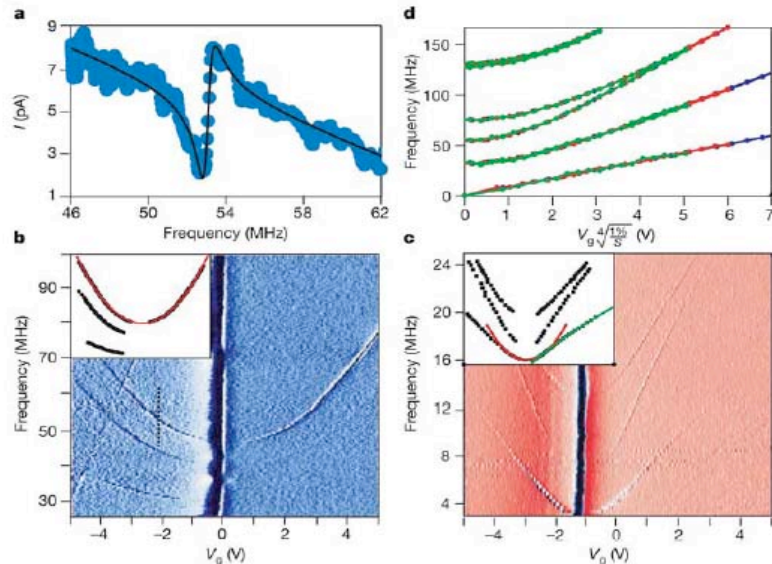


**Figure 2** Measurements of the resonant response. The measurements were done on 11 devices, both semiconducting and small bandgap semiconducting nanotubes in a vacuum chamber at pressures below  $10^{-4}$  torr. The maximum conductance  $G^{\text{max}}$ , and the transconductance  $dG/dV_g^{\text{max}}$ , are given below for the presented devices. **a**, Detected current as a function of driving frequency taken at  $V_g = 2.2\text{ V}$ ,  $\delta V_g = 7\text{ mV}$  for device 1 ( $G^{\text{max}} = 12.5\ \mu\text{S}$ ,  $dG/dV_g^{\text{max}} = 7\ \mu\text{S V}^{-1}$ ). The solid black line is a lorentzian fit to the data with an appropriate phase shift between the driving voltage and the oscillation of the tube. The fit yields the resonance frequency  $f_0 = 55\text{ MHz}$ , and quality factor  $Q = 80$ . **b**, **c**, Detected current (plotted as a derivative in colour scale) as a function of gate voltage and frequency for devices 1 and 2 ( $G^{\text{max}} = 10\ \mu\text{S}$ ,  $dG/dV_g^{\text{max}} = 0.3\ \mu\text{S V}^{-1}$ ). Panel **a** is

a vertical slice through panel **b** at  $V_g = 2.2\text{ V}$  (marked with a dashed black line). The insets to the figures show the extracted positions of the peaks in the frequency–gate voltage space for the respective colour plots. A parabolic and a  $V_g^{2Q}$  fit of the peak position are shown in red and green, respectively. **d**, Theoretical predictions for the dependence of vibration frequency on gate voltage for a typical device with length  $L = 1.75\ \mu\text{m}$ , and radius  $r = 1\text{ nm}$ . The calculations were performed for several different values of slack  $s$  ( $s = (L - W)/W$ , where  $L$  is the tube’s length and  $W$  is the distance between clamping points). The calculations for 0.5%, 1% and 2% slack are shown in blue, red and green, respectively. Notice the appropriately rescaled x-axis.

<i>Tersoff-Brenner parameter set-1</i>	<i>Extensional Stiffness (N/m)</i>	<i>Torsional Stiffness (N/m)</i>	<i>Tersoff-Brenner parameter set-2</i>	<i>Extensional Stiffness (N/m)</i>	<i>Torsional Stiffness (N/m)</i>
(9,6) Chiral	121.016	35.674	(9,6) Chiral	157.292	41.811
(5,5) Armchair	120.023	35.797	(5,5) Armchair	156.014	41.815
(10,0) Zigzag	117.375	19.392	(10,0) Zigzag	152.356	21.579

Table 1. Values of extensional and torsional moduli for 3 different CNTs, and the two sets of Tersoff-Brenner parameters.

semi-conducting and small band gap semi-conducting carbon nanotubes are used to detect the vibrational motion of the CNT.

Experimental results for the measured current as a function of driving frequency at room temperature appear in Figure 2a. Figures 2b and 2c show the measured response as a function of the driving frequency and the static gate voltage. The resonant frequency shifts upwards with increase of the magnitude of the DC voltage. Several different vibrational modes of the CNT are observed. Finally, simulated results for a representative device are shown in Figure 2d. The frequency dependence of the resonances is in good qualitative agreement with theoretical predictions.

### 3. Phonon-phonon interactions and clamping losses:

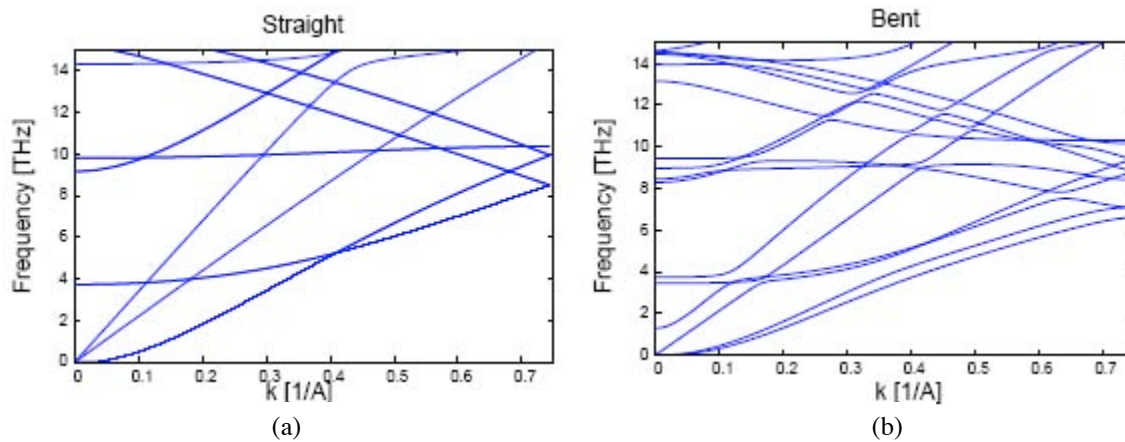


Figure 3. Dispersion relations for (a) straight and (b) bent nanotubes.

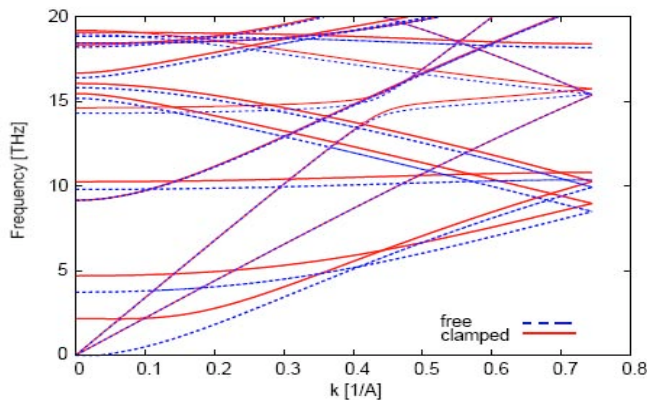


Figure 4. Dispersion relations for free and clamped nanotubes.

The main vibration mode (acoustic mode) of a nano oscillator interacts with the thermally distributed vibration modes of the system. This interaction results in energy loss. Energy can also be lost at the clamped ends of a nano oscillator. These loss mechanisms are under current investigation. This analysis is being carried out by expanding the Hamiltonian of the system around its equilibrium configuration. The scattering rate of the acoustic phonon is calculated by Fermi's

Golden Rule. Preliminary results appear in Figures 3-4. Figures 3a and 3b show dispersion relations for a straight nanotube as well as a nanotube that is bent into a torus. Gaps are seen to open up in Figure 3(b) at points where the different branches of the dispersion curves intersect. The magnitudes of these gaps, as functions of the radius of curvature, are needed to determine the phonon scattering rate.

Figure 4 compares the dispersion relations of a free nanotube with that of a clamped one. It is seen that the wave vector changes very little for the higher frequency modes, thus indicating that this loss mechanism should be important in these modes. In contrast, clamping losses should be negligible for the transverse acoustic mode. Therefore, it is possible to create high quality factor devices that operate in this regime.

#### 4. Detailed BEM/FEM model for vibration of nanotubes:

Work is in progress on a detailed Boundary Element – Finite Element (BEM-FEM) model for simulating vibrations of a nanotube. The FEM will be used to model a nanotube as a beam and the BEM will be used to model the exterior electric field. Analogous work on MEMS plate vibrations and on thin plate MEMS has recently been carried out on this project [5-8].

Preliminary results from BEM calculations for the charge distribution around a nanotube appear in Figures 5a and 5b. As expected, the charge distribution is nearly axisymmetric when the gap is large and is asymmetric when the gap is small. The traction at a point on the nanotube outer surface is proportional to the square of the charge density and is directed radially outwards.

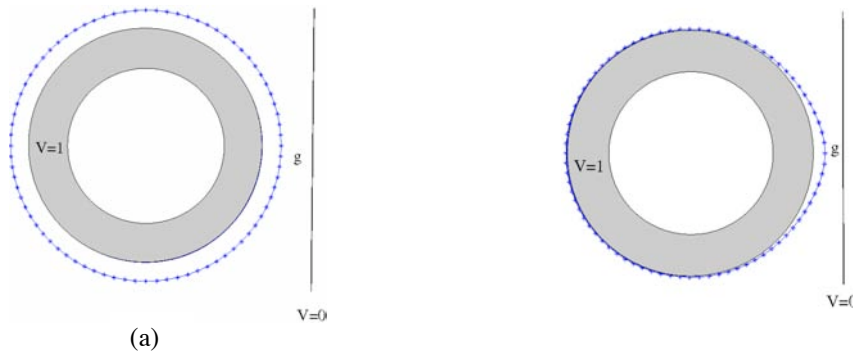


Figure 5. Charge distribution  $\rho(r, \theta)$  around a nanotube with inner and outer radii  $a=0.665$  nm and  $b=1$  nm. (a) Large gap  $g=250$  nm. (b) Small gap  $g=0.1$  nm. The actual difference between  $\rho_{\max}$  and  $\rho_{\min}$  in (a) is about 1% of  $\rho_{\max}$ .

#### Future work

Ongoing work involves detailed simulation of vibration of carbon nanotubes, calculation of losses and further experiments. An enriched continuum model is being implemented in order to simulate more realistic behavior of vibrating CNTs. The last task in this project involves the building of CNT devices. A tunable CNT oscillator has already been presented in [4] and also in this report. Other examples of devices that will be tried are ultrasensitive force and mass detectors. From the start, this project has been a close collaborative effort between the mechanics and physics groups at Cornell, and this will continue during the rest of this project.

## References

- [1] K. Chandraseker and S. Mukherjee. Extension, torsion and bending of single-walled carbon nanotubes, under preparation.
- [2] P. Zhang, Y. Huang, P.H. Geubelle, P.A Klein, K.C. Hwang. The elastic modulus of single-wall carbon nanotubes: a continuum analysis incorporating interatomic potentials. *International Journal of Solids and Structures* 39, 2002, pp. 3893-3906.
- [3] R. Saito, G. Dresselhaus, M. S. Dresselhaus. Physical properties of carbon nanotubes. *Imperial College Press*, London, 1998.
- [4] V. Sazonova, Y. Yaish, H. Ustunel, D. Roundy, T. A. Arias, P. L. McEuen. A tunable carbon nanotube electromechanical oscillator. *Nature*, Vol. 431, 2004, pp. 284-287.
- [5] Z. Bao, S. Mukherjee, M. Roman and N. Aubry, Nonlinear vibrations of beams, strings, plates and membranes without initial tension. *ASME Journal of Applied Mechanics*, Vol. 71, 2004, pp. 551-559.
- [6] S. Mukherjee, Z. Bao, M. Roman and N. Aubry, Nonlinear mechanics of MEMS plates with a total Lagrangian approach. *Computers and Structures*. In press.
- [7] Z. Bao and S. Mukherjee, Electrostatic BEM for MEMS with thin conducting plates and shells. *Engineering Analysis with Boundary Elements*. Vol. 28, 2004, pp. 1427-1435.
- [8] Z. Bao and S. Mukherjee, Electrostatic BEM for MEMS with thin beams. *Communications in Numerical Methods in Engineering*. In press.